AFRL-RZ-WP-TP-2008-2033

SECONDARY BREAKUP OF AERATED LIQUID JETS IN SUBSONIC CROSSFLOW (POSTPRINT)

B. Miller, K.A. Sallam, M. Bingabr, K.-C. Lin, and C. Carter

Propulsion Sciences Branch
Aerospace Propulsion Division

FEBRUARY 2008
Interim Report

Approved for public release; distribution unlimited.

See additional restrictions described on inside pages

STINFO COPY

AIR FORCE RESEARCH LABORATORY
PROPULSION DIRECTORATE
WRIGHT-PATTERSON AIR FORCE BASE, OH 45433-7251
AIR FORCE MATERIEL COMMAND
UNITED STATES AIR FORCE

REPORT DOCUMENTATION PAGE

Form Approved
OMB No. 0704-0188

1. REPORT DATE *(DD-MM-YY)*	2. REPORT TYPE	3. DATES COVERED *(From - To)*
February 2008	Conference Paper Postprint	30 April 2006 – 01 December 2006

4. TITLE AND SUBTITLE
SECONDARY BREAKUP OF AERATED LIQUID JETS IN SUBSONIC CROSSFLOW (POSTPRINT)

5a. CONTRACT NUMBER
IN HOUSE

5b. GRANT NUMBER

5c. PROGRAM ELEMENT NUMBER
61102F

6. AUTHOR(S)
B. Miller and K.A. Sallam (Oklahoma State University)
M. Bingabr (University of Central Oklahoma)
K.-C. Lin (Taitech Inc.)
C. Carter (Propulsion Sciences Branch, Aerospace Propulsion Division (AFRL/RZAS)

5d. PROJECT NUMBER
2308

5e. TASK NUMBER
AI

5f. WORK UNIT NUMBER
2308AI00

7. PERFORMING ORGANIZATION NAME(S) AND ADDRESS(ES)
Propulsion Sciences Branch
Aerospace Propulsion Division
Air Force Research Laboratory, Propulsion Directorate
Wright-Patterson Air Force Base, OH 45433-7251
Air Force Materiel Command, United States Air Force

Oklahoma State University
University of Central Oklahoma
Taitech Inc.

8. PERFORMING ORGANIZATION REPORT NUMBER
AFRL-RZ-WP-TP-2008-2033

9. SPONSORING/MONITORING AGENCY NAME(S) AND ADDRESS(ES)
Air Force Research Laboratory
Propulsion Directorate
Wright-Patterson Air Force Base, OH 45433-7251
Air Force Materiel Command
United States Air Force

10. SPONSORING/MONITORING AGENCY ACRONYM(S)
AFRL/RZAS

11. SPONSORING/MONITORING AGENCY REPORT NUMBER(S)
AFRL-RZ-WP-TP-2008-2033

12. DISTRIBUTION/AVAILABILITY STATEMENT
Approved for public release; distribution unlimited.

13. SUPPLEMENTARY NOTES
PAO case number AFRL/WS06-2863, 22 December 2006. ©2007 K.A. Sallam. Presented at the 45th AIAA Aerospace Sciences Meeting and Exhibit, 8-11 January 2007, Reno, NV. The U.S. Government is joint author of the work and has the right to use, modify, reproduce, release, perform, display, or disclose the work. Document contains color.

14. ABSTRACT
An experimental investigation of the secondary breakup of an aerated liquid jet in subsonic crossflow is described. The present test conditions were similar to those encountered in fuel injection in ramjet engines. Previous studies of spray structures of aerated liquid jet in crossflow have been limited to the dilute spray area (downstream distance > 100 jet diameter) using Phase Doppler Particle Analyzer (PDPA) and along the liquid surface using wet-holographic plates. The objective of the present study was to extend these earlier measurements to investigate the dense spray near-injector region immediately downstream of the injector (0-50 jet diameter) where secondary breakup occurs in order to bridge the gap between drop size distribution along the jet surface and those obtained using PDPA in the far-field of the injector. Three-dimensional microscopic digital holography was used to record and measure droplets sizes and locations within the three-dimensional volume of the spray. The test conditions include different gas-to-liquid mass flow rate ratios and jet-to-free stream momentum flux ratios.

15. SUBJECT TERMS

16. SECURITY CLASSIFICATION OF: a. REPORT	b. ABSTRACT	c. THIS PAGE	17. LIMITATION OF ABSTRACT:	18. NUMBER OF PAGES	19a. NAME OF RESPONSIBLE PERSON (Monitor)
Unclassified	Unclassified	Unclassified	SAR	18	Campbell D. Carter

19b. TELEPHONE NUMBER *(Include Area Code)*
(937) 255-7328

Standard Form 298 (Rev. 8-98)
Prescribed by ANSI Std. Z39-18

AIAA 2007-1342

AIAA-2007-1342

Secondary Breakup of Aerated Liquid Jets in Subsonic Crossflow

B. Miller[1] and K. A. Sallam[2]
Oklahoma State University, Stillwater, OK, 74078

M. Bingabr[3]
University of Central Oklahoma, Edmond, OK 73034

K.-C. Lin[4]
Taitech Inc., Beavercreek, OH 45433

C. Carter[5]
Air Force Research Laboratory, Wright-Patterson AFB, OH 45433

An experimental investigation of the secondary breakup of an aerated liquid jet in subsonic crossflow is described. The present test conditions were similar to those encountered in fuel injection in ramjet engines. Previous studies of spray structures of aerated liquid jet in crossflow have been limited to the dilute spray area (downstream distance > 100 jet diameter) using Phase Doppler Particle Analyzer (PDPA) and along the liquid surface using wet-holographic plates. The objective of the present study was to extend these earlier measurements to investigate the dense spray near-injector region immediately downstream of the injector (0-50 jet diameter) where secondary breakup occurs in order to bridge the gap between drop size distribution along the jet surface and those obtained using PDPA in the far-field of the injector. Three dimensional microscopic digital holography was used to record and measure droplets sizes and locations within the three dimensional volume of the spray. Earlier results of the primary breakup of aerated liquid jets in crossflow show that the gas jet along the axis of the annular flow leaving the injector passage forces the annular liquid sheet into a conical shape that extends from the injector exit. Primary breakup occurs in a similar manner along both the upstream and downstream sides of the liquid jet (relative to the crossflow) which suggests relatively weak aerodynamic effects on the primary breakup. In the present study the aerodynamic effects on the drop sizes in the wake region of the fuel injector were considered. The test conditions include different gas-to-liquid mass flow rate ratios and jet-to-free stream momentum flux ratios. The present measurements of the spray structure of aerated liquid jets in crossflows shows a reduction in drop sizes with downstream distance due to the drop secondary breakup.

Nomenclature

Alphabetical

d	= *drop diameter*
d_0	= *injector orifice diameter*
d_L	= *liquid sheet thickness, Eq. (1)*
GLR	= *aerating gas-to-liquid mass flow rate ratio*
h	= *spray plume penetration height*
h_0	= *non-aerated spray plume penetration height*
M	= *Mach number*

[1] Graduate Student.
[2] Assistant Professor, Member AIAA. Corresponding author; Tel: 405-762-0749, Fax: 405-744-7873, Email: khaled.sallam@okstate.edu (K.A. Sallam).
[3] Assistant Professor.
[4] Senior Research Scientist, Associate Fellow AIAA.
[5] Senior Aerospace Engineer, Member AIAA.

MMD	= *mass median diameter*
Q	= *volumetric flow rate*
Q_G	= *volumetric flow rate of gas injected*
Q_L	= *volumetric flow rate of liquid injected*
q	= *jet/freestream momentum flux ratio* $\rho_L^2\ v_j^2 / \rho_\infty u_\infty^2$
q_0	= *non-aerated jet/freestream momentum flux ratio*
SMD	= *Sauter mean diameter,* $\sum d_i^3 / \sum d_i^2$, *i for all droplets*
u	= *velocity component in the crossflow (horizontal) direction*
u_∞	= *freestream velocity*
v	= *velocity component in jet streamwise (vertical) direction*
w	= *width of the spray plume*
x	= *cross-stream (horizontal) distance from the injector exit*
y	= *streamwise (vertical) distance from the injector exit*
z	= *span wise (normal to the page) distance from the injector exit*

Greek

β	= *flow-average void fraction, Eq. (2)*
ρ	= *density*

Subscripts

0	= *property at GLR = 0*
G	= *aerating gas property*
j	= *jet exit property*
L	= *liquid property*
∞	= *ambient gas property*

I. Introduction

Aerated injection is characterized by injecting a gas phase and a liquid phase together within the injector. At low gas-to-liquid mass flow rate ratios (GLR), the flow will exit the injector as a liquid jet with gas bubbles in the center of the jet. At higher GLR, however, the flow will exit as an annular flow consisting of a thin liquid film surrounding a gas core. The spray produced in the annular regime is made up of densely packed small droplets. This property of the spray makes it very useful for many applications, especially ramjet and scramjet applications,[1] but it makes analyzing the spray difficult. Studies of spray structure have been performed downstream in the less dense region using Phase Doppler Particle Anemometry (PDPA) by Lin et al.[2-4] The properties at the injector exit were also measured by Sallam et al.[5] They found that the underexpanded gas jet at the exit of the sonic (choked) injector passage forces the annular liquid sheet into a conical shape that extends from the injector exit. Primary breakup occurs along that liquid sheet in a similar manner along both the upstream and downstream sides of the liquid jet (relative to the crossflow) which suggests that there are relatively weak aerodynamic effects on the primary breakup. The secondary breakup in the near injector region was not considered in this study. This leaves a gap of information about the aerodynamic effects on drop sizes between the less dense downstream area in the far field and the injector exit. This region is characterized by non-spherical droplets that are packed closely together. These non-spherical droplets prohibit the use of PDPA in this area, and shadowgraphy is only able to capture a few droplets in focus due to the limited depth of field associated with the high levels of magnification needed to measure the small droplets encountered in the spray. Holography techniques, however, ease the limitation on the depth of field and allow three-dimensional volumes of the spray at different locations to be measured. Therefore, a digital holographic technique was used in the present study to penetrate this dense spray region and measure these non-spherical droplets. The objectives of this study were to use a digital holographic technique to create three-dimensional maps of droplet sizes, which was used to observe the effects of different injection parameters on droplets sizes. The parameters studied were: gas-to-liquid mass flow rate ratio (GLR), jet-to-freestream momentum ratio, and injector diameter. Changes in droplet sizes with downstream distance were measured to investigate whether or not secondary breakup might be occurring.

II. Experimental Methods

A. Apparatus

Aerated-liquid injectors with exit diameters of 0.5 mm and 1.0 mm were used. These injectors consist of an inner tube for the aerating gas and an outer tube for the liquid, as shown in Fig. 1. The aerated liquid jets were injected into a subsonic wind tunnel with a test section of 0.3 m × 0.3 m × 0.6 m as shown in Fig. 2. The wind tunnel had float glass side walls and floor, and acrylic ceiling to provide optical access. The air velocities in the test section were in the range of 3-60 m/s at normal temperature and pressure. The air velocity in the test section, was measured by a Pitot-static tube (United Sensors Model PDC-18-G-16-KL) installed at the end of the test section. The Pitot-static tube was connected to an inclined tube manometer (Dwyer Model No. 400-10-Kit). Air velocities in the wind tunnel could be measured within ± 2%. The wind tunnel had a contraction ratio greater than 16:1 and the velocity variation inside the test section was < ± 1% of mean free-stream velocity. The test liquid was contained within a cylindrical liquid supply chamber having a diameter of 100 mm and a length of 300 mm, constructed of type 304 stainless steel. The liquid was forced through the injector by admitting high-pressure air to the top of the chamber. The aerating gas travels through the inner tube and passes through several 100-μm holes located near the end of the tube. At sufficient GLRs (greater than 2%) the gas and liquid mix to form a two-phase flow which consists of a gas core surrounded by a thin liquid sheet (annular regime). The air and liquid flow rates were then controlled by rotameter type flow meters (air flow meter: OMEGA model # 044-40NCA, water flow meter: OMEGA model # N034-39G). The air flow meter could read flow rates ±3 cc/s and the water flow meter could read flow rates ±0.02 cc/s. The uncertainty in the flow rate measurement is 6%. The high-pressure air was kept in a storage tank with a volume of 0.18 m^3 and provided an injection pressure of 1.1 MPa.

B. Instrumentation

Two methods of digital holography were considered, in-line digital holography and digital holographic microscopy. In previous work in this lab[6] in-line digital holography was chosen to study the spray of aerated injectors because of its ability to capture a large field of view and its experimental setup simplicity. This technique, however, would not provide the resolution required to resolve the smallest droplets in the spray. For higher magnification, but smaller field of view, digital holographic microscopy[7] was used. This technique removes some of the lenses that were necessary in the in-line setup, which greatly reduces the number of aberrations introduced by lenses. The optical setup was similar to Miller et al.[6] except that only one beam was used that was expanded with a 5x objective lens, and then passed directly through the test section to a Cooke Corporation cooled interline transfer CCD camera (Cooke, Model: PCO 2000) having 2048 × 2048 pixels that were 7.4 μm wide by 7.4 μm tall.

After the hologram is recorded, as shown in Fig. 3(a), it is reconstructed, as shown in Fig. 3(b), using the convolution type approach which solves the Rayleigh Sommerfeld formula for reconstruction of a wave field by the use of the Fast Fourier Transform algorithm.[8] The method of average intensity subtraction is used in the current hologram reconstruction, and the current setup neglects the out-of-focus virtual image since its effect is small enough that droplets can still be resolved and measured accurately. Using this method the smallest measurable droplets with diameters of 17 μm were measured with uncertainties of 50%. However, the majority of the droplets measured were near the SMD size. The smallest SMD size was 59 μm. Droplets of this size could be measured with uncertainty of 15%. Irregular drops were assumed to be ellipsoids and were assigned diameters equal to the diameter of the sphere having the same volume as the ellipsoid. Reconstructions were made with 1 mm increments, and hence the location of the centroid of the droplet can be known within ±1 mm. Measurements in the x and y direction were determined by the placement of the camera when the holograms were recorded. The placement of the camera could be determined ±2 mm.

III. Results and Discussion

The results of this study are presented as three-dimensional maps of the SMD for different test conditions as shown in Tables 1 and 2. The orientation of these maps is similar to Fig. 2. The results of SMD are summarized in Table 3.

A. Effect of GLR

Changing the GLR had the most effect over the droplet sizes. Figure 4 shows this effect. The SMD for the entire population at the condition of d_0=1 mm and q_0=0.74, is reduced from 151 μm to 71 μm when the GLR is

increased from 4% to 8%. This is due to the liquid film being "squeezed" into a thinner sheet due to the increased gas flow rate. The equation that describes this liquid film thickness is given by Lin et al.[2] as follows:

$$d_L = d_0(1-\beta^{1/2})/2 \tag{1}$$

where d_0 is the nozzle exit diameter and β is the flow-average void fraction given by Lin et al.[2] as:

$$\beta = Q_G/(Q_G+Q_L) \tag{2}$$

In this equation the variables Q_G and Q_L are the volumetric flow rates of the gas and liquid, respectively. If the SMD is normalized by this film thickness, which is controlled by the GLR, the values will be on the same order of magnitude. This shows that the droplet size is not controlled by the jet diameter but by the GLR which controls the film thickness.

The penetration height of the spray plume is also affected by different GLRs. When comparing the two different GLRs in Fig. 4, the 8% GLR condition results in a height difference of 15 jet diameters. This is due to the thinner liquid sheet exiting the injector at a higher velocity than the thicker liquid sheet at the lower GLR. A correlation for this height has been reported by Lin et al.[4]:

$$(h-h_0)/d_0 = 0.9(GLR)^{0.46}M^{-0.64}q_0^{\ 0.34}(x/d_0)^{0.39} \tag{3}$$

where

$$h_0/d_0 = 3.17q_0^{\ 0.33}(x/d_0)^{0.40} \tag{4}$$

Here h is the penetration height, h_0 is the non-aerated penetration height, q_0 is the jet-to-freestream momentum ratio, and M is the freestream Mach number. The predicted penetration heights given by this correlation are listed in Table 1 and Table 2 with the measured values in the present study. The difference between the two may be attributed to the fact that in Lin et al.[4] the penetration heights in the far field ($x/d_0>100$) are determined using a threshold of 0.01 cc/s/cm^2 whereas in the present measurements the location of the highest drop in the spray at that downstream location was taken as the penetration height. The present measurements of h/d_0 listed in Table 1 and Table 2 are therefore labeled as the maximum h/d_0.

Lin et al.[4] stated that the GLR has little effect on the width of the spray plume. This also holds true in the current results. The correlation given for the width of the spray plume, w, is given[4] as:

$$w/2d_0 = 3.07q_0^{\ 0.10}(x/d_0)^{0.45} \tag{5}$$

These predicted values are listed in Table 1 and Table 2 along with the present measurements. The present measurements are the maximum width of the spray so they are expected to be larger than the predicted value which defines the edge of the spray as the place where the volume flux is greater than 0.01 cc/s/cm^2.

B. Effect of Jet Exit Diameter

When the spray produced by the 1 mm injector is compared with the 0.5 mm injector, the effects on the drop size are small similar to earlier observations in the far field ($x/d_0>100$) by Lin et al. [4]. These effects can be seen in Table 3. The SMD distribution of the sprays remained relatively constant when only the jet exit diameter was changed. This is most likely due to the fact that the droplet size is controlled more by the thickness of the liquid sheet exiting the injector which is controlled by the GLR, than the physical size of the jet diameter. The most significant effect the jet diameter had on the spray was on the number of droplets that were observed for the same test conditions. While the SMD distribution of the spray remained relatively constant the number of the droplets observed in the case of the large injector was nearly double the number of droplets for the small injector. This is due to the fact that the flow rate of the liquid that was injected using the smaller injector (Q_L=0.33 cc/s)) was lower than the flow rate of the liquid being injected into the larger injector (Q_L=1.45 cc/s). This was done so that the q_0 would remain constant for different jet diameters.

C. Effect of Jet/Freestream Momentum Flux Ratio

The main effect of the jet/freestream momentum flux ratio was controlling the spray plume penetration, which agrees with the findings of Lin et al.[1-4] The two jet/freestream momentum flux ratios investigated were q_0=0.74 and q_0=4. This effect can be seen in Fig. 5. As expected the q_0=4 condition provided larger penetration heights than the q_0=0.74 condition. The jet/freestream momentum flux ratio also has an effect on the spray plume width. As predicted by Eq. (5), as q_0 increases so does the spray plume width. It can be seen from Table 1 and Table 2 that at the higher values of q_0 the spray plume is wider than at similar conditions with a lower value of q_0.

D. Effect of Downstream Location

Major changes in droplet sizes as they travel downstream imply that secondary breakup occurred between the two locations. It is expected that the droplet diameters should shrink some amount as they travel downstream due to evaporation, but large changes may indicate that something else is taking place, namely secondary breakup. The measured values of overall SMD are listed in Table 3. At the 8% GLR conditions there is little or no change between the two downstream distances, but at the all of the 4% GLR conditions there is a considerable reduction in SMD of up to 60 μm. This could be evidence of secondary breakup in this region. To determine if secondary breakup is occurring, the droplets velocities should be measured and the droplets Weber number should be calculated in the questionable region. According to Hsiang and Faeth[9] drops will begin breaking up at Weber number around 10. Other properties such as spray plume penetration and spray plume width are also being affected by downstream distance. It is evident the spray is continuing to increase in height and width as it travels from x/d_0=25 to x/d_0=50. This means that the droplets are still retaining their initial momentum and did not relax to the local conditions.

E. Overall Droplet Distribution

Simmons[10] showed that a universal linear correlation for drop-size/volume-fraction distributions of sprays can be established for all fuel nozzles if the drop sizes are normalized by their mass median diameter (MMD) and plotted on a root-normal scale. Using this correlation the volume-fractions corresponding to any drop-size range can be estimated given the MMD or the SMD. Figure 6 shows the present data plotted according to Simmons.[10] It can be seen that the majority of these data points at GLR=8% follows Simmons' universal root normal distribution with MMD/SMD=1.2. However, for some of the test conditions of 4% GLR the values fall below this line.

V. Conclusions

The present work has managed to probe the spray of aerated injectors in subsonic crossflow in the optically challenging near injector area. The present study found evidence of secondary breakup in some of the test conditions. The major conclusions are as follows:

1. Digital holography is a useful tool for examining this dense near injector area and can provide information other methods can not. This is due to the fact that it is insensitive to the droplets being non-spherical in this region.
2. Digital holographic microscopy works better than the standard digital in-line holography.[6] It removes a substantial amount of noise because of the elimination of the additional lenses needed with the in-line method.
3. As the GLR increased from 4% to 8% droplet sizes decreased. The droplet sizes were independent of other variables such as injector diameter. Jet-to-freestream momentum flux ratio had little effect on droplet size. Drop sizes were found to correlate with the film thickness which is a function of the GLR.
4. Reductions in droplet sizes at the GLR=4% conditions between the two downstream locations of x/d_0=25 and x/d_0=50 showed signs of secondary breakup. Further investigation of the droplets Weber numbers is needed.

Acknowledgments

Support from Tiatech Inc. under a subcontract with the Air Force Research Laboratory and from NASA Oklahoma space grant fellowship for the first author (B. Miller) is gratefully acknowledged. Initial development of experimental methods was carried out under the National Science Foundation, Grant No. EPS-0132534 (Oklahoma-

EPSCOR). The U.S. Government is authorized to make copies of this article for governmental purposes notwithstanding any copyright notation thereon.

References

[1]Lin, K.-C., Kennedy, P.J. and Jackson, T.A., "Penetration Heights of Liquid Jets in High-Speed Crossflows," *40th AIAA Aerospace Sciences Meeting and Exhibit*, 2002.

[2]Lin, K.-C., Kirkendall, K.A., Kennedy, P.J. and Jackson, T.A., "Spray Structures of Aerated Liquid Fuel Jets in Supersonic Crossflows," *35th AIAA/ASME/SAE/ASEE Joint Propu `lsion Conference and Exhibit*, 2374, 1999, 1-11.

[3]Lin, K.-C., Kennedy, P.J. and Jackson, T.A., "Spray Structures of Aerated-Liquid Jets in Subsonic Crossflows," *32nd AIAA Aerospace Sciences Meeting*, 3178, 2001, 1-18.

[4]Lin, K.-C., Kennedy, P.J. and Jackson, T.A., "Structures of Aerated Liquid Jets in High Speed Crossflows," *32nd AIAA Fluid Dynamics Conference*, 3178, 2002, 1-12.

[5]Sallam, K.A., Aalburg, C., Faeth, G.M., Lin, K.-C., Carter, C.D. and Jackson, T.A., "Primary Breakup of Round Aerated-Liquid Jets in Supersonic Crossflows," *Atomization and Sprays*, 16(6), 2006, 657-672.

[6]Miller, B., Sallam, K.A., Lin, K.-C. and Carter, C., "Digital Holographic Spray Analyzer," *ASME Joint U.S.-European Fluids Engineering Summer Meeting*, FEDSM2006-98526, 2006.

[7]Schnars, U. and Jueptner, W. *Digital Holography: Digital Hologram Recording, Numerical Reconstruction, and Related Techniques*. (Springer, Berlin, 2005).

[8]Kreis, T.M., Adams, M. and Jüptner, W.P., "Methods of Digital Holography: A Comparison," *SPIE*, 3098, 1997, 224-233.

[9]Hsiang, L.-P. and Faeth, G.M., "Drop Deformation and Breakup due to Shock Wave and Steady Disturbances," *International Journal of Multiphase Flow*, 21(4), 1995, 545-560.

[10]Simmons, H.C., "The Correlation of Drop-Size Distributions in Fuel Nozzle Sprays," *Journal of Engineering for Power*, 99(3), 1977, 309-319.

Table 1 Summary of results for 0.5 mm injector

d_0 (mm)	0.5	0.5	0.5	0.5	0.5	0.5	0.5	0.5
M (-)	0.16	0.16	0.16	0.16	0.07	0.07	0.07	0.07
x/d_0 (-)	25	50	25	50	25	50	25	50
q_0 (-)	0.74	0.74	0.74	0.74	4	4	4	4
GLR (%)	4	4	8	8	4	4	8	8
Q_L (cc/s)	0.33	0.33	0.33	0.33	0.33	0.33	0.33	0.33
Q_G (cc/s)	10.8	10.8	21.7	21.7	10.8	10.8	21.7	21.7
SMD (μm)	154	97	75	62	168	149	74	70
h / d_0 from Lin et al.[4] (-)	38	50	45	59	89	117	109	143
Present maximum h / d_0 (-)	60	90	60	90	120	180	120	180
$w / 2d_0$ from Lin et al.[4] (-)	12.7	17.3	12.7	17.3	15	20.5	15	20.5
Present maximum $w / 2d_0$ (-)	22	22	17	22	22	30	24	28

Table 2 Summary of results for 1.0 mm injector

d_0 (mm)	1.0	1.0	1.0	1.0	1.0	1.0	1.0	1.0
M (-)	0.18	0.18	0.18	0.18	0.075	0.075	0.075	0.075
x/d_0 (-)	25	50	25	50	25	50	25	50
q_0 (-)	0.74	0.74	0.74	0.74	4	4	4	4
GLR (%)	4	4	8	8	4	4	8	8
Q_L (cc/s)	1.45	1.45	1.45	1.45	1.45	1.45	1.45	1.45
Q_G (cc/s)	49	49	103	103	49	49	103	103
SMD (μm)	151	118	72	59	164	106	86	73
h / d_0 from Lin et al.[4] (-)	27	35	33	43	68	90	87	115
Present maximum h / d_0 (-)	45	60	60	75	105	120	90	120
$w / 2d_0$ from Lin et al.[4] (-)	12.7	17.3	12.7	17.3	15	20.5	15	20.5
Present maximum $w / 2d_0$ (-)	12.5	18.5	14.5	21	19.5	25	21.5	25.5

Table 3 Drop size reduction between x/d_0 = 25 and 50 for each of the test conditions

d_0 (mm)	GLR	q_0	v_∞ (m/s)	v_{jet} (m/s)	x/d_0	SMD (μm)	Reduction in SMD
1	4%	0.74	61	64	25	151	
1	4%	0.74	61	64	50	118	22%
1	4%	4	26	64	25	164	
1	4%	4	26	64	50	106	35%
0.5	4%	0.74	56	56	25	154	
0.5	4%	0.74	56	56	50	97	37%
0.5	4%	4	24.2	56	25	168	
0.5	4%	4	24.2	56	50	149	11%
1	8%	0.74	61	133	25	72	
1	8%	0.74	61	133	50	59	18%
1	8%	4	26	133	25	86	
1	8%	4	26	133	50	73	15%
0.5	8%	0.74	56	112	25	75	
0.5	8%	0.74	56	112	50	62	17%
0.5	8%	4	24.2	112	25	74	
0.5	8%	4	24.2	112	50	70	5%

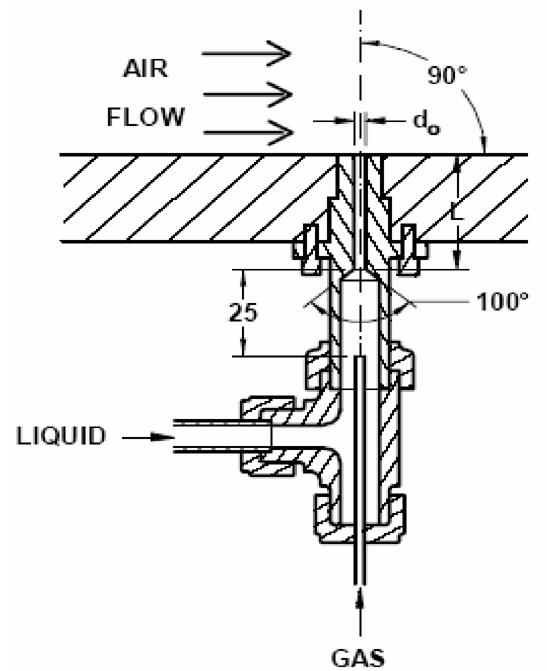

Figure 1 Schematic of an aerated injector (inside out setup shown) (from reference [3]).

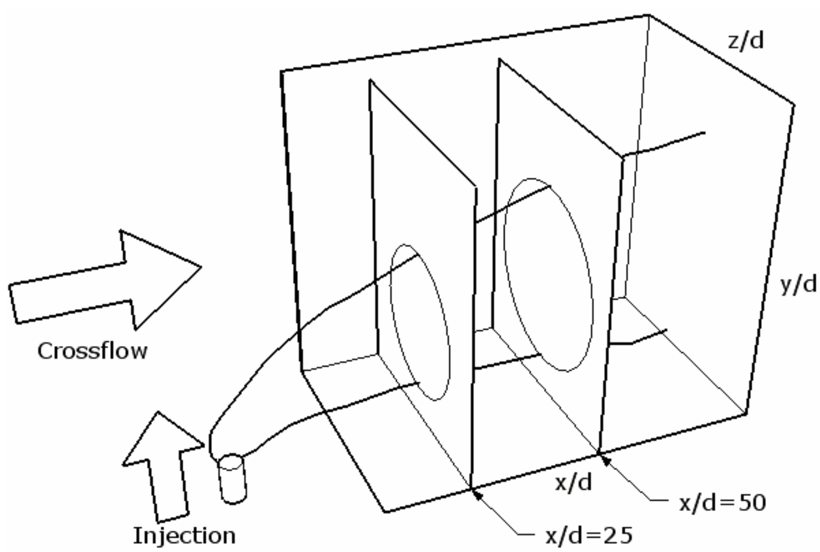

Figure 2 Sketch showing the orientation of the SMD plots.

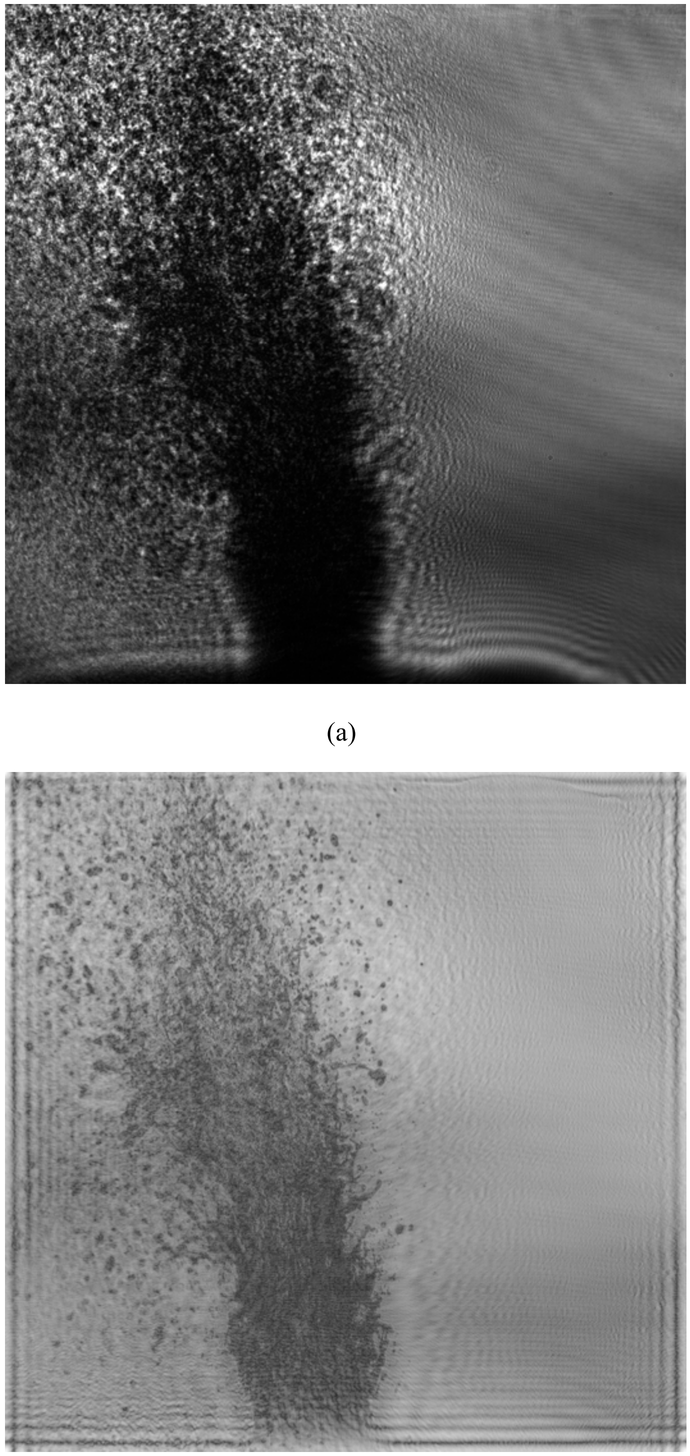

(a)

(b)

Figure 3 (a) Hologram recorded using digital holographic microscopy at the injector exit with test conditions of GLR=4%, q_0 = 0.74, and d_0 = 1 mm (the gaseous crossflow is from right to left). (b) Reconstruction of the hologram at the jet plan of symmetry.

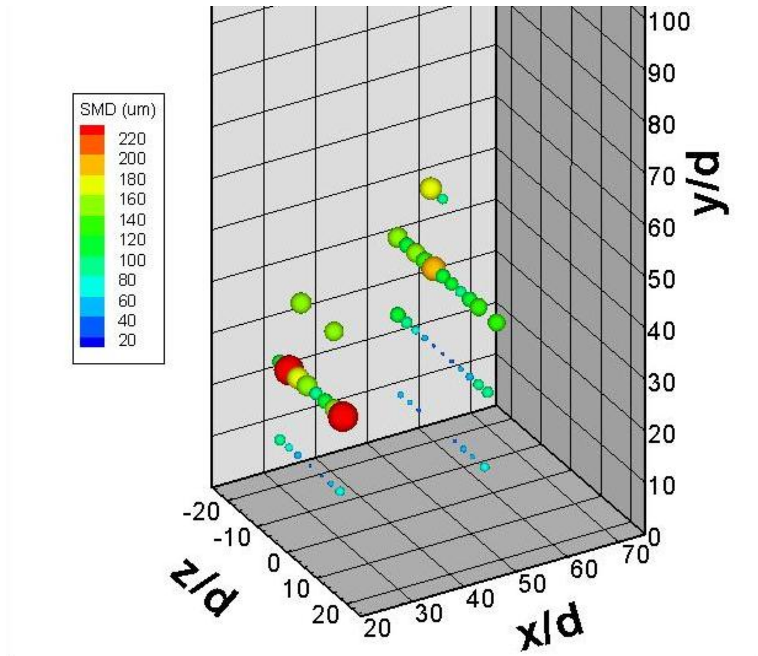

(a)

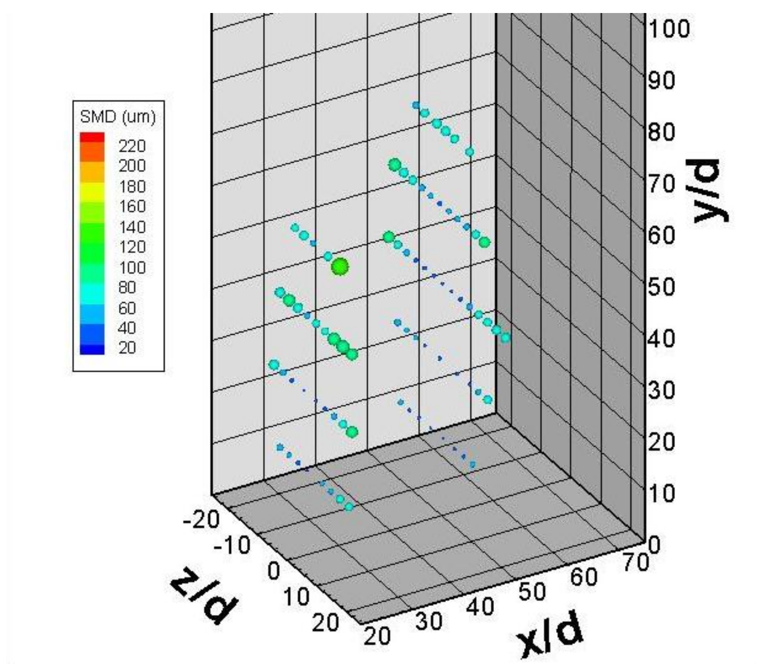

(b)

Figure 4 Effect of GLR: (a) SMD Distribution at GLR=4%, q_0=0.74, and d_0=1 mm and (b) SMD Distribution at GLR=8%, q_0=0.74, and d_0=1 mm

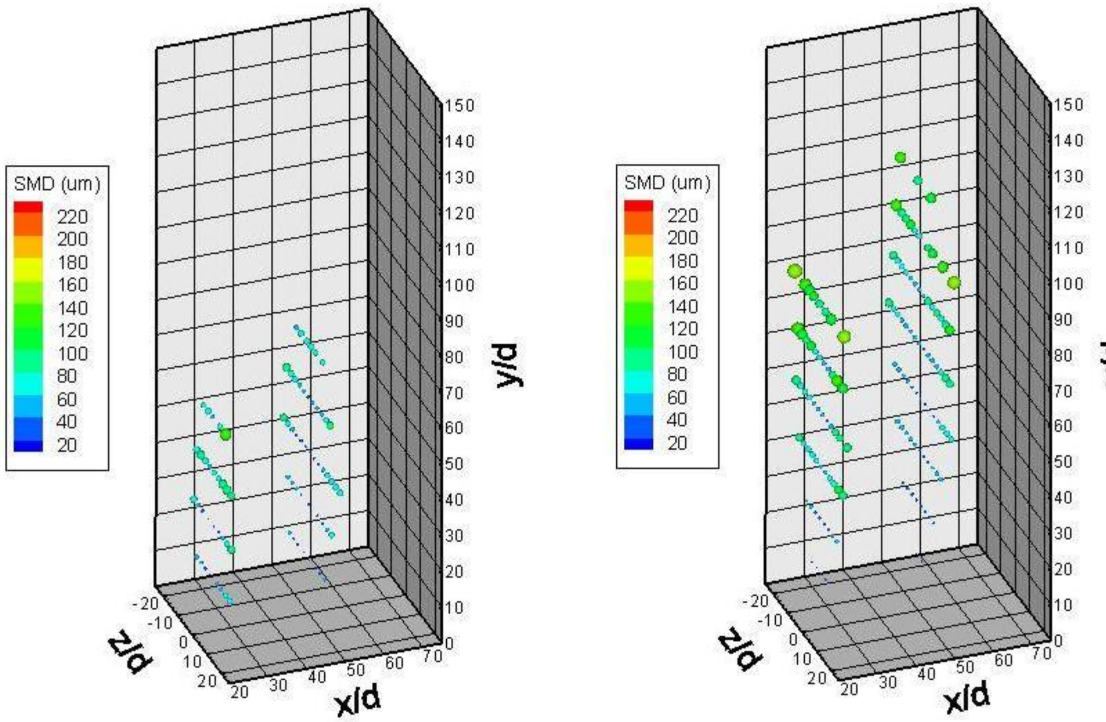

(a) (b)

Figure 5 Effect of q_0: (a) SMD Distribution at GLR=8%, q_0=0.74, and d_0=1 mm and (b) SMD Distribution at GLR=8%, q_0=4, and d_0=1 mm.

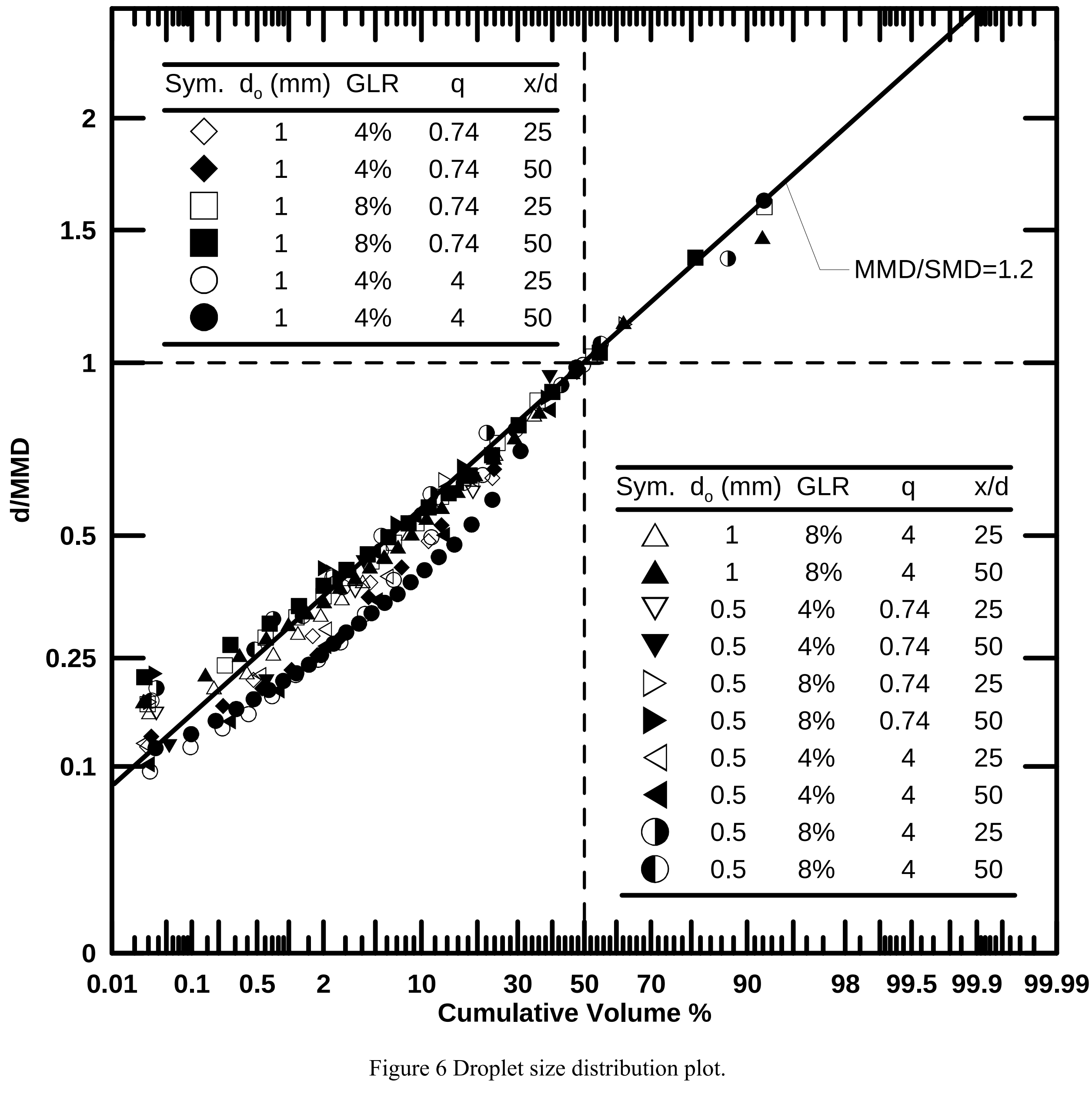

Figure 6 Droplet size distribution plot.